


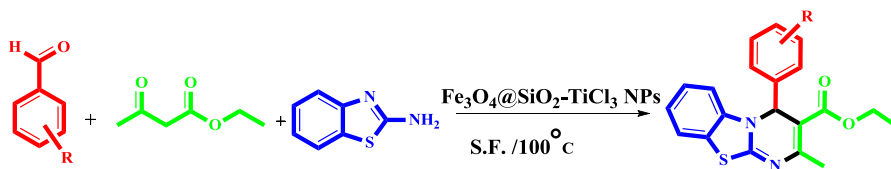
# Nano- $\text{Fe}_3\text{O}_4@\text{SiO}_2\text{-TiCl}_3$ as a novel nano-magnetic catalyst for the synthesis of 4*H*-pyrimido[2,1-*b*]benzothiazoles

Seyede Azita Fazeli-Attar<sup>1</sup> · Bi Bi Fatemeh Mirjalili<sup>1</sup> 

Received: 18 March 2018 / Accepted: 31 May 2018  
© Springer Nature B.V. 2018

**Abstract**  $\text{Fe}_3\text{O}_4@\text{SiO}_2\text{-TiCl}_3$  NPs, a novel core shell catalyst, was synthesized via preparing  $\text{Fe}_3\text{O}_4@\text{SiO}_2$  as a magnetic support followed by treatment with titanium tetrachloride ( $\text{TiCl}_4$ ). The structure, morphology and magnetic properties of this catalyst were recognized by different techniques including Fourier transform infrared spectroscopy, field emission scanning electron microscopy, X-ray diffraction, vibrating sample magnetometry as well as thermo-gravimetric analysis. To consider the catalytic activity of this magnetic catalyst, it was used in a multicomponent reaction between 2-aminobenzothiazole, aldehydes and ethyl acetoacetate to synthesize 4*H*-pyrimido[2,1-*b*]benzothiazole derivatives. Our results indicated that the compounds were synthesized with high yield and purity in a short reaction time. Furthermore, the obtained results indicated that this catalyst can be reused for at least three times without no significant change in the efficiency.

## Graphical Abstract



**Electronic supplementary material** The online version of this article (doi:<https://doi.org/10.1007/s11164-018-3498-6>) contains supplementary material, which is available to authorized users.

✉ Bi Bi Fatemeh Mirjalili  
fmirjalili@yazd.ac.ir

<sup>1</sup> Department of Chemistry, College of Science, Yazd University, P.O. Box 89195-741, Yazd, Islamic Republic of Iran

**Keywords** Nano- $\text{Fe}_3\text{O}_4@\text{SiO}_2\text{-TiCl}_3$  · 4*H*-pyrimido[2,1-*b*]benzothiazole · Solid acid catalyst · Solvent free condition · Multicomponent reaction

## Introduction

Among heterocyclic compounds, fused heterocycles showed a substantial role in pharmaceutical industry [1]. Benzothiazole derivatives were categorized as the fused heterocycles. They have been known to have significant applications in development of medicinal chemistry [2, 3]. To synthesis the pharmaceutical compounds, it is necessary to use a convenient and straightforward method without extra purification. The 4*H*-pyrimido[2,1-*b*]benzothiazole derivatives are compounds with the potential ability in the preparation of drugs. In recent years, these compounds were known to be functioning as anti-tumor [4], anti-inflammatory [5], anti-bacterial and anti-fungal [6] materials. The synthesis of 4*H*-pyrimido[2,1-*b*]benzothiazole is a three-component condensation reaction between aldehyde,  $\beta$ -ketoester and 2-aminobenzothiazole. The catalysts including  $\text{Fe}_3\text{O}_4$ @nano-cellulose- $\text{TiCl}$  [7], nano- $\text{TiCl}_2$ /cellulose [8],  $\text{PdCl}_2$  [9], C-Ti  $\text{O}_2\text{-SO}_3\text{-SbCl}_2$  [10], chitosan [11], *N*-sulfonic acid modified poly(styrene-maleic anhydride) SMI- $\text{SO}_3\text{H}$  [12],  $\text{FeF}_3$  [13], tetrabutylammonium hydrogen sulfate (TBAHS) [14], hydrotalcite [15],  $\text{AlCl}_3$  [16] and 1,1,3,3-*N,N,N,N'*-tetramethylguanidinium trifluoroacetate (TMGT) [17] have recently been applied to synthesis of these compounds. To reduce disadvantages of some of these catalysts, a new and powerful catalyst was prepared in this study. Our results showed that this catalyst was also stable and friendly to the environment.

In recent years, the heterogeneous catalysts in organic reactions have been extremely interesting. They showed the advantages including simple product separation and purification steps as well as simplicity of their storage and handling. Researchers have tried to improve these catalysts through decrease of their size, increase of their surface areas and activity. Nanoparticles (NPs) were known as the intermediate of homogeneous and heterogeneous catalysts that can be efficiently dispersed in the reaction medium and then, improved the reaction [18]. However, these catalysts had a small size, and; therefore, their separation was difficult. Therefore, magnetic nanoparticles (MNPs) have been selected as the catalyst support [19–22]. These nanoparticles can be easily separated from reaction medium by an external magnet without using extra chemicals [23].

To control the oxidation and aggregation of these magnetic nanoparticles, the surfaces of  $\text{Fe}_3\text{O}_4$  nanoparticles were coated [24]. In recent years, different coatings for  $\text{Fe}_3\text{O}_4$  nanoparticles have been applied. They included surfactants [25], biopolymers [7, 22, 26], silica [19, 21] and carbon [27–29]. The studies indicated that a silica coating showed the efficient properties including nontoxicity, excellent biocompatibility, stability and ability to be grafted with different modifiers. These characteristics have caused the ( $\text{Fe}_3\text{O}_4@\text{SiO}_2$ ) core-shell structure to have more attention and applied as a catalyst [21, 23, 24]. In the present study,  $\text{Fe}_3\text{O}_4@\text{SiO}_2\text{-TiCl}_3$  NPs was used as a powerful and ecofriendly catalyst. Its effect was assessed in

the reaction of ethyl acetoacetate, aldehydes and 2-amino benzothiazole for the synthesis of 4*H*-pyrimido[2,1-*b*]benzothiazole.

## Experimental

### General

All compounds were purchased from Merck, Aldrich and Fluka chemical companies and used without any additional purification. FT-IR spectra were run on a Bruker, Equinox 55 spectrometer. The Bruker (DRX-400 Avance) NMR was used to record the  $^1\text{H}$ -NMR spectrum. Melting points were determined by a Buchi melting point B-540 B.V.CHI apparatus and were uncorrected. The X-ray diffraction (XRD) pattern was obtained by a Philips Xpert MPD diffractometer equipped with a Cu Ka anode ( $k = 1.54 \text{ \AA}$ ) in the  $2\theta$  range from  $10^\circ$  to  $80^\circ$ . Field emission scanning electron microscopy (FESEM) photographs were obtained on a Mira 3-XMU. Transmission electron microscopy (TEM) photographs were recorded by a Leo 912AB OMEGA instrument. The XRF analysis was done with a Bruker, S4 Explorer instrument. The VSM measurements were performed by using a Vibrating Sample Magnetometer (Meghnatis Daghigh Kavir Co. Kashan Kavir, Iran).

### Preparation of $\text{Fe}_3\text{O}_4$ NPs

A mixture of  $\text{FeCl}_2 \cdot 4\text{H}_2\text{O}$  (1 g, 5 mmol) and  $\text{FeCl}_3 \cdot 6\text{H}_2\text{O}$  (2.7 g, 10 mmol) was dissolved in deionized water (25 mL) and heated in a water bath until the temperature was  $80^\circ\text{C}$ . Then, 17 mL of  $\text{NH}_3$  (30%) was added drop wise and stirred by using a mechanical stirrer. After stirring the mixture for 30 min, the black magnetic nanoparticles were aggregated by an external magnet, washed with distilled water three times and dried at  $80^\circ\text{C}$  for 2 h.

### Preparation of $\text{Fe}_3\text{O}_4@\text{SiO}_2$

At first, the mixture of 1.4 g of  $\text{Fe}_3\text{O}_4$  NPs in 10 mL of ethanol and 3 mL of  $\text{NH}_3$  (35%) (mixture A), were sonicated in an ultrasonic bath for 30 min. Then, the solution of 0.85 mL of  $\text{Si}(\text{OEt})_4$  in 10 mL of ethanol was added drop wise to the mixture A and stirred by using a mechanical stirrer for 1 h at room temperature. Finally, the obtained mixture was filtrated and washed with ethanol.

### Preparation of $\text{Fe}_3\text{O}_4@\text{SiO}_2\text{-TiCl}_3$ NPs

To obtain the mixture of  $\text{Fe}_3\text{O}_4@\text{SiO}_2$  (1.7 g) in dichloromethane (10 mL),  $\text{TiCl}_4$  (1.7 mL) was added drop wise and stirred in a well-ventilated system for 1 h at room temperature. After removing HCl, the mixture was filtered and washed with dichloromethane to remove unreacted  $\text{TiCl}_4$  and dried at room temperature to obtain  $\text{Fe}_3\text{O}_4@\text{SiO}_2\text{-TiCl}_3$  NPs.

## General procedure for the synthesis of 4*H*-pyrimido[2,1-*b*]benzothiazole derivatives

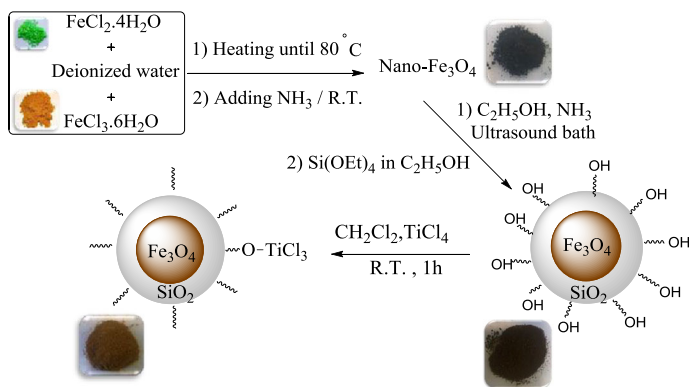
In a 25 ML round bottom flask, aldehyde (1 mmol), ethyl acetoacetate (1 mmol), 2-aminobenzothiazole (1 mmol) and  $\text{Fe}_3\text{O}_4@\text{SiO}_2\text{-TiCl}_3$  NPs (0.04 g) were charged. The obtained mixture was heated to 100 °C in an oil bath and stirred by a mechanical stirring motor with a speed of 50 rpm. The progress of the reaction was monitored by TLC. After completing the reaction, the reaction mixture was dissolved in ethanol. The catalyst was separated by using an external magnet and then water was added to the solution. A pure solid appeared in high yield.

## Results and discussion

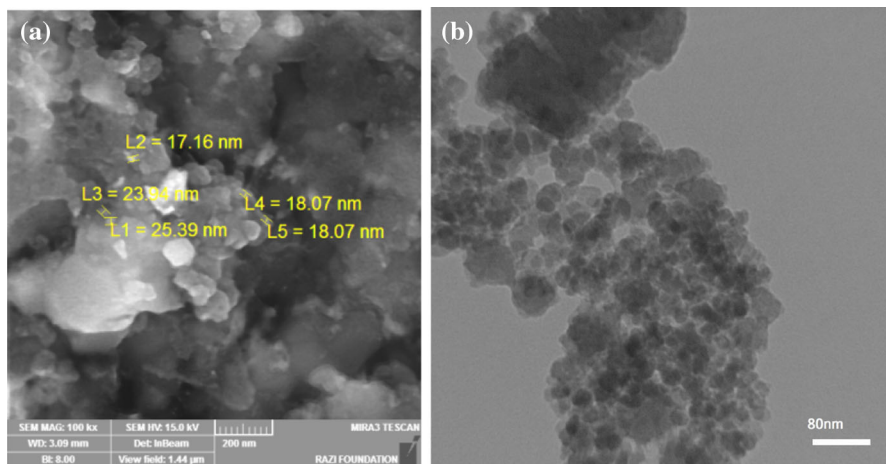
To synthesize  $\text{Fe}_3\text{O}_4@\text{SiO}_2\text{-TiCl}_3$  NPs as a new catalyst,  $\text{Fe}_3\text{O}_4@\text{SiO}_2$  were prepared by using the pre-prepared nano- $\text{Fe}_3\text{O}_4$  and  $\text{Si}(\text{OEt})_4$ . Then,  $\text{TiCl}_4$  was added to  $\text{Fe}_3\text{O}_4@\text{SiO}_2$ . This process led to generation of this acidic heterogeneous catalyst (scheme 1).

Field emission scanning electron microscopy (FESEM) and transmission electron microscopy (TEM) were used to provide more accurate information about the particle size of the catalyst. As the results obtained from TEM and FESEM showed, the dimensions of  $\text{Fe}_3\text{O}_4@\text{SiO}_2\text{-TiCl}_3$  NPs were almost 20 nm (Fig. 1).

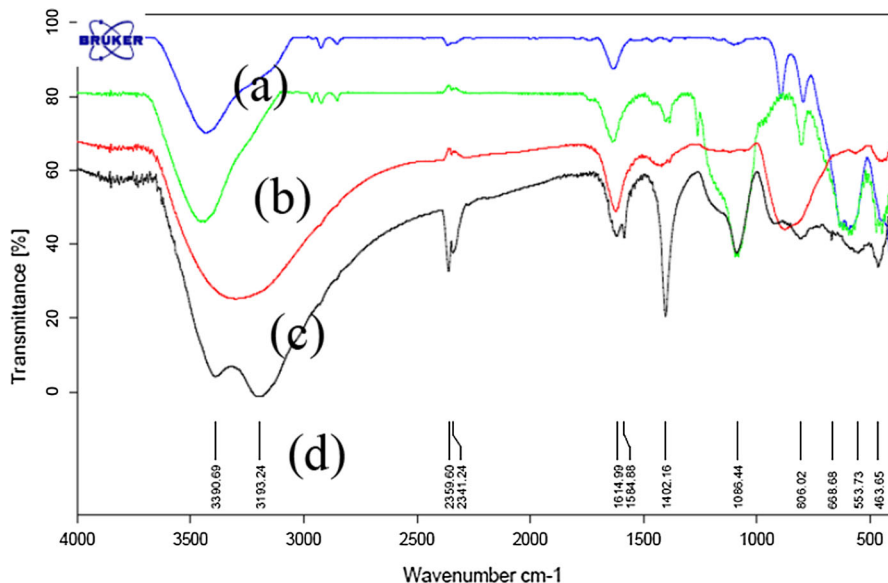
To study the structure of  $\text{Fe}_3\text{O}_4@\text{SiO}_2\text{-TiCl}_3$  NPs, the FT-IR spectrum of  $\text{Fe}_3\text{O}_4@\text{SiO}_2\text{-TiCl}_3$  NPs (d) was measured and compared with the FT-IR spectra of nano- $\text{Fe}_3\text{O}_4$ (a),  $\text{Fe}_3\text{O}_4@\text{SiO}_2$  (b) and  $\text{TiCl}_4$  (c) (Fig. 2). The peaks observed at 463 and 554  $\text{cm}^{-1}$  are attributed to Fe/O in  $\text{Fe}_3\text{O}_4$  nanoparticles [30]. After coating the surface of  $\text{Fe}_3\text{O}_4$  with  $\text{SiO}_2$ , the appearance of two signals at 1088 and 806  $\text{cm}^{-1}$  exhibited asymmetric and symmetric stretching vibration of a Si–O–Si bond, respectively. The stretching and bending vibrations of the O–H bond were visible at 3388 and 1617  $\text{cm}^{-1}$ , respectively. It is notable that the Fe/O–Si band was appeared



**Scheme 1** Preparation of  $\text{Fe}_3\text{O}_4@\text{SiO}_2\text{-TiCl}_3$  NPs



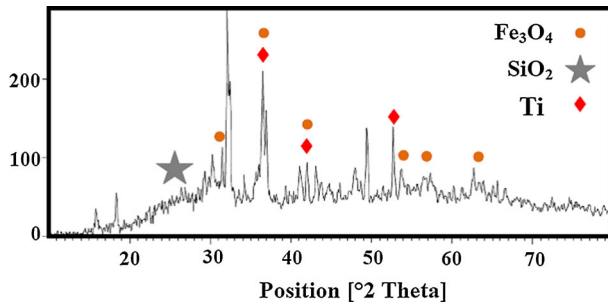
**Fig. 1** **a** FESEM and **b** TEM image of Fe<sub>3</sub>O<sub>4</sub>@SiO<sub>2</sub>-TiCl<sub>3</sub> NPs



**Fig. 2** FT-IR spectra of (a) nano-Fe<sub>3</sub>O<sub>4</sub>, (b) Fe<sub>3</sub>O<sub>4</sub>@SiO<sub>2</sub>, (c) TiCl<sub>4</sub> and (d) Fe<sub>3</sub>O<sub>4</sub>@SiO<sub>2</sub>-TiCl<sub>3</sub> NPs

at approximately 584 cm<sup>-1</sup> which overlapped with the Fe/O signal. In the spectrum of the catalyst, the Si-O-Ti peak at 940–960 cm<sup>-1</sup> indicated titanium successfully bonded to the surface of SiO<sub>2</sub>.

Figure 3 shows the X-ray diffraction (XRD) pattern of the Fe<sub>3</sub>O<sub>4</sub>@SiO<sub>2</sub>-TiCl<sub>3</sub> NPs. The values of 2θ and FWHM are recorded in Table 1. The peaks at 2θ of 31.07°, 36.51°, 42.00°, 53.80°, 56.82° and 63.03° were consistent with FWHM of 2.5190, 0.2362, 0.2362, 0.2362, 1.8893 and 2.3040, respectively. These



**Fig. 3** The XRD pattern of  $\text{Fe}_3\text{O}_4@\text{SiO}_2\text{-TiCl}_3$

**Table 1**  $\text{Fe}_3\text{O}_4@\text{SiO}_2\text{-TiCl}_3$  NPs reflexes in XRD diffractogram

No.	Pos. ( $^{\circ}2\theta$ )	FWHM ( $^{\circ}2\theta$ )
1	15.7764	0.3149
2	18.3811	0.2362
3	31.0748	2.5190
4	32.1442	0.3149
5	36.5149	0.2362
6	42.0020	0.2362
7	49.4550	0.2362
8	52.7252	0.2362
9	53.8054	0.2362
10	56.8205	1.8893
11	63.0364	2.3040

observations confirmed the crystalline cubic spinel structure of  $\text{Fe}_3\text{O}_4$  nanoparticles [31]. The broad peak observed at  $2\theta$  of  $20^{\circ}$ – $30^{\circ}$  range described amorphous  $\text{SiO}_2$  [32]. Presumably, three other peaks in  $2\theta$  of  $36.51^{\circ}$ ,  $42.00^{\circ}$  and  $53.8^{\circ}$  revealed that Ti was bonded to  $\text{SiO}_2$ .

The X-ray fluorescence (XRF) analysis was used to measure the chemical composition of catalyst (Table 2). The comparison between Kilo Counts Per Seconds (KCPS) values of Ti and Cl in XRF catalyst and KCPS values of the same elements in pure  $\text{TiO}_2$  and NaCl showed that the amount of Ti and Cl 4.2 g

**Table 2** The XRF analysis of catalyst and pure samples of NaCl and  $\text{TiO}_2$

Elemental component	$\text{Fe}_3\text{O}_4@\text{SiO}_2\text{-TiCl}_3$		NaCl		$\text{TiO}_2$	
	KCPS	wt%	KCPS	wt%	KCPS	wt%
Cl	82.9	11.1	516.5	62		
$\text{TiO}_2$	162.7	15.5			2318.4	60
$\text{SiO}_2$	41.9	18.6				
$\text{Fe}_2\text{O}_3$	819.5	56				

(0.088 mol) and 10 g (0.28 mol), respectively. These results indicated that Ti:Cl ratio is approximately 1:3 in  $\text{Fe}_3\text{O}_4@\text{SiO}_2\text{-TiCl}_3$ .

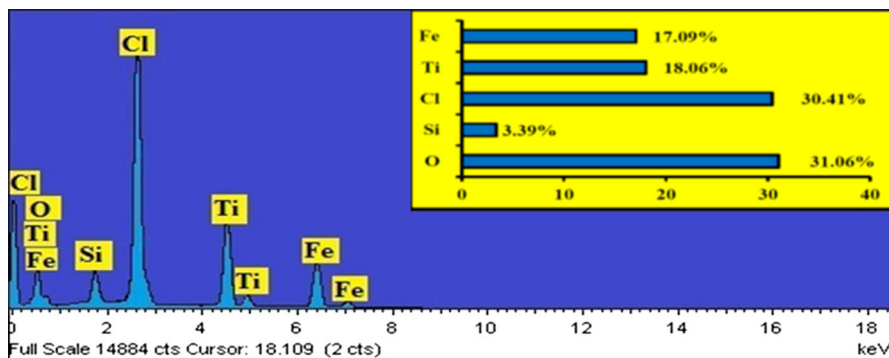
The components of the  $\text{Fe}_3\text{O}_4@\text{SiO}_2\text{-TiCl}_3$  NPs were analyzed using energy-dispersive X-ray spectroscopy (EDX) analysis (Fig. 4). The peaks of Fe, O, Si, Cl and Ti were observed and the compositions of  $\text{Fe}_3\text{O}_4@\text{SiO}_2\text{-TiCl}_3$  NPs were reported to be 17.09, 31.06, 3.39, 30.41 and 18.06% for Fe, O, Si, Cl and Ti, respectively.

The thermal gravimetric analysis (TG–DTA) pattern of  $\text{Fe}_3\text{O}_4@\text{SiO}_2\text{-TiCl}_3$  NPs was also performed through heating from 100 to 800 °C (Fig. 5). According to the curves, the 4% weight loss in the temperature 80–100 °C can be attributed to the water desorption (exothermic). Two subsequent weight losses of the catalyst corresponded to 10 and 2% in the temperature 100–400 °C and 400–800 °C, respectively (endothermic). These observations showed that the catalyst was stable till 100 °C. The char yield of catalyst at 800 °C is 86% of original sample weight.

Brunauer–Emmett–Teller (BET) theory was applied to measure the specific surface area of the catalyst. The single point surface area was  $2.73 \text{ m}^2 \text{ g}^{-1}$  at  $P/P_0 = 0.984$ , while the measured mean pore diameter and the total pore volume were 9.5287 nm and  $6.5119 \times 10^{-3} \text{ cm}^3 \text{ g}^{-1}$ , respectively. The  $\text{N}_2$  adsorption isotherm of catalyst is shown in Fig. 6.

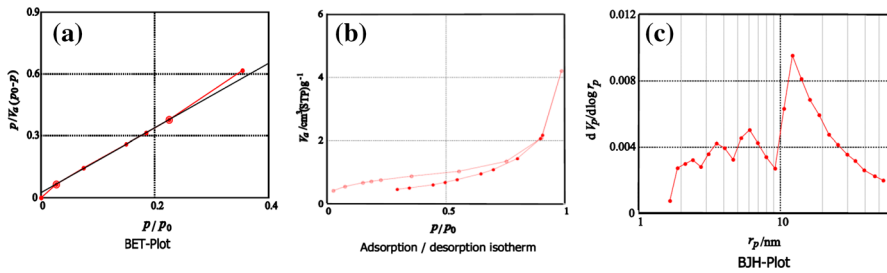
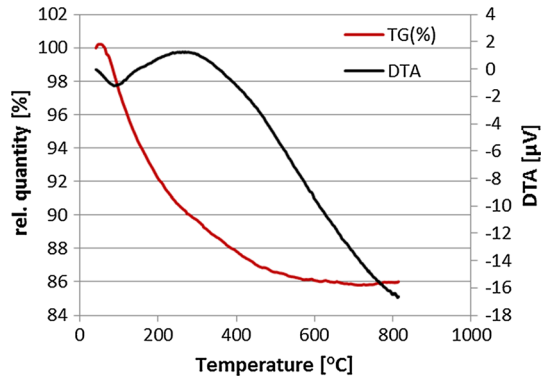
The magnetic property of  $\text{Fe}_3\text{O}_4@\text{SiO}_2\text{-TiCl}_3$  NPs was evaluated by a vibrating sample magnetometer (VSM) at room temperature (Fig. 7). The figure shows that the catalyst ( $\text{Fe}_3\text{O}_4@\text{SiO}_2\text{-TiCl}_3$  NPs) was superparamagnetic. The results indicated that the coercivity value was zero, and there was no hysteresis loop and remanence. The saturation magnetization (Ms) values of  $\text{Fe}_3\text{O}_4$  and  $\text{Fe}_3\text{O}_4@\text{SiO}_2\text{-TiCl}_3$  NPs were 46.67 and  $6.67 \text{ emu g}^{-1}$ , respectively. Although the magnetization of  $\text{Fe}_3\text{O}_4$  decreased after coating, the catalyst can be easily separated from the solution with an external magnet.

After discovering the catalyst's characteristics, the reaction of ethylacetoacetate, benzaldehyde and 2-aminobenzothiazole was chosen as the model reaction to



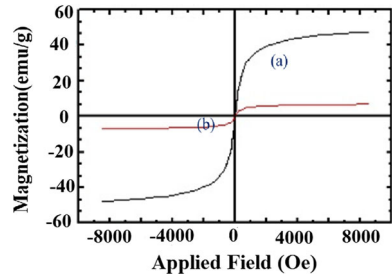
**Fig. 4** The EDX spectra of  $\text{Fe}_3\text{O}_4@\text{SiO}_2\text{-TiCl}_3$  NPs

**Fig. 5** The thermal gravimetric analysis pattern of  $\text{Fe}_3\text{O}_4@\text{SiO}_2\text{-TiCl}_3$  NPs



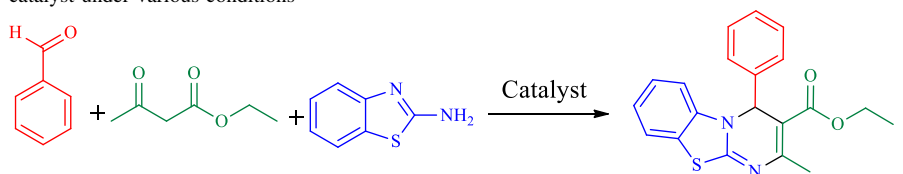
**Fig. 6** **a** BET (Brunauer–Emmett–Teller), **b** adsorption/desorption isotherm and **c** BJH (Barrett–Joyner–Halenda) plots of  $\text{Fe}_3\text{O}_4@\text{SiO}_2\text{-TiCl}_3$  NPs

**Fig. 7** Magnetization loops of (a)  $\text{Fe}_3\text{O}_4@\text{SiO}_2\text{-TiCl}_3$  NPs and (b)  $\text{Fe}_3\text{O}_4$

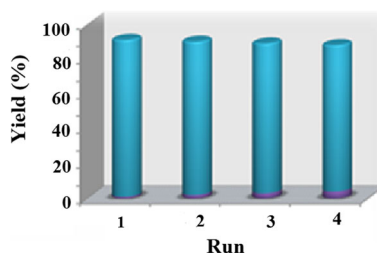


evaluate its catalytic activity and the reaction conditions. The results are presented in Table 3. After evaluating of the reaction medium and selecting a solvent free condition as the best medium, the effect of different temperatures and amounts of catalysts were checked. Then, the amount 0.04 g of the catalyst at 100 °C was selected.

The reusability is one of the most important qualities of a catalyst. Therefore, after using the catalyst in the model reaction, it was separated by an external magnet, washed by chloroform and then, dried. The results obtained from reusing

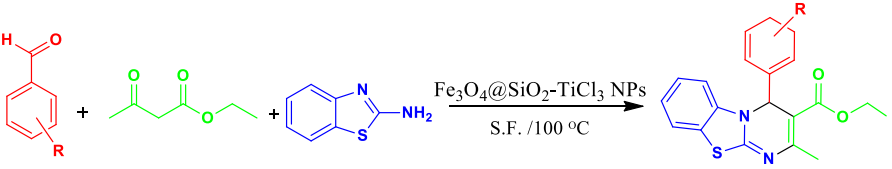
**Table 3** The reaction of 2-aminobenzothiazole, benzaldehyde and ethyl acetoacetate in the presence of catalyst under various conditions<sup>a</sup>

Entry	Catalyst <sup>b</sup> (g)	Solvent/condition	Time (min)/yield (%) <sup>c</sup>
1	0.04	H <sub>2</sub> O/reflux	180/–
2	0.04	C <sub>2</sub> H <sub>5</sub> OH/reflux	180/–
3	0.04	Acetonitrile/reflux	180/50
4	0.04	–70 °C	150/71
5	0.04	–80 °C	150/90
6	0.04	–90 °C	75/70
7	0.04	–100 °C	45/90
8	0.04	–110 °C	30/70
9	0.04	–120 °C	40/73
10	0.02	–100 °C	45/61
11	0.03	–100 °C	45/68
12	0.05	–100 °C	45/54

<sup>a</sup>The molar ratio of 2-aminobenzothiazole:benzaldehyde:ethyl acetoacetate is 1:1:1<sup>b</sup>Fe<sub>3</sub>O<sub>4</sub>@SiO<sub>2</sub>-TiCl<sub>3</sub> NPs<sup>c</sup>Isolated yield**Fig. 8** The reusability of the catalyst

the catalyst showed no significant loss of its catalytic activity after four times (Fig. 8).

To establish the catalytic activity, other 4*H*-pyrimido[2,1-*b*]benzothiazole derivatives were synthesized by using different aromatic aldehydes under optimized conditions. According to Table 4, aldehydes carrying electron-withdrawing groups showed more reactivity than aldehydes with electron-donating groups.

**Table 4** The synthesis of 4*H*-pyrimido[2,1-*b*]benzothiazole derivatives<sup>a</sup>


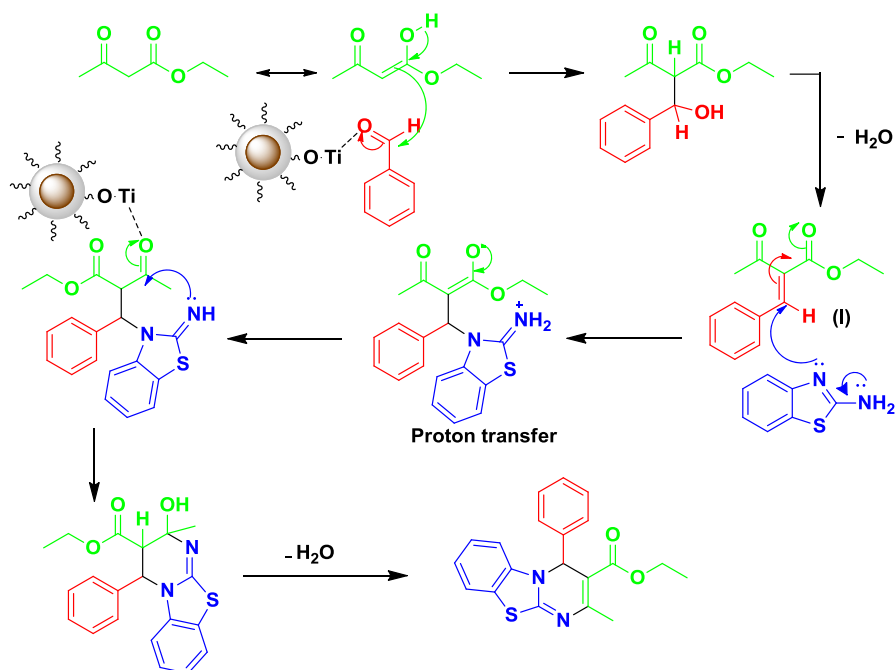
Entry	R	Time (min)	Yield (%) <sup>b</sup>	M.P. (ref.)
1	H	45	90	175–178 [14]
2	4-NO <sub>2</sub>	60	88	153–156 [17]
3	4-Cl	120	83.6	140–142
4	4-Br	150	84	107–109 [17]
5	4-OH	35	79	218–222
6	2-NO <sub>2</sub>	45	89	160–164
7	2-Cl	120	90	130–132 [14]
8	3-NO <sub>2</sub>	40	83.6	218–220 [7]
9	3-OH	90	87.7	259–261 [8]
10	2,4-(Cl) <sub>2</sub>	120	82	112–116
11	2,4-(OMe) <sub>2</sub>	120	83	164–166
12	3,4-(OH) <sub>2</sub>	25	83	227–229 [7]

<sup>a</sup>The molar ratio of 2-aminobenzothiazole:aldehyde:ethyl acetoacetate is 1:1:1<sup>b</sup>Isolated yield

A plausible mechanism for the reaction of ethylacetoacetate, aldehyde and 2-aminobenzothiazole was outlined in scheme 2. At first, the carbonyl groups in aldehyde and  $\beta$ -ketoester have been bonded to Ti in catalyst and activated for further condensation. Condensation of activated aldehyde and  $\beta$ -ketoester was done by the Knoevenagel reaction and produced compound (I). Then, 2-aminobenzothiazole reacted with compound (I) through a Michael addition to make an iminium ion. After proton transferring and cyclization, 4*H*-pyrimido[2,1-*b*]benzothiazole compounds were formed.

## Conclusions

In summary, we have described the preparation and characterization of Fe<sub>3</sub>O<sub>4</sub>@-SiO<sub>2</sub>-TiCl<sub>3</sub> NPs as a novel, powerful and ecofriendly heterogeneous catalyst. This catalyst showed excellent catalytic activity in a multicomponent reaction for the synthesis of 4*H*-pyrimido[2,1-*b*]benzothiazoles. Some significant advantages of this protocol were high yield, short reaction time, easy work-up, facile separation and reusability of the catalyst.



**Scheme 2** A proposed mechanism for preparation of 4*H*-pyrimido[2,1-*b*]benzothiazole derivatives

**Acknowledgements** The Research Council of Yazd University is gratefully acknowledged for the financial support for this work.

## References

1. Y.D. Gong, T. Lee, J. Comb. Chem. **12**, 393 (2010)
2. S. Seth, Antiinflamm. Antiallergy Agents Med. Chem. **14**, 98 (2015)
3. P. Chander Sharma, K. Kumar Bansal, A. Deep, M. Pathak, Curr. Top. Med. Chem. **17**, 208 (2017)
4. M.T. Gabr, N.S. El-Gohary, E.R. El-Bendary, M.M. El-Kerdawy, Eur. J. Med. Chem. **85**, 576 (2014)
5. S. Nalawade, V. Deshmukh, S. Chaudhari, J. Pharm. Res. **7**, 433 (2013)
6. M.S. Chaitanya, G. Nagendrappa, V.P. Vaidya, J. Chem. Pharm. Res. **2**, 206 (2010)
7. S. Azad, B.F. Mirjalili, RSC Adv. **6**, 96928 (2016)
8. S. Azad, B.F. Mirjalili, Res. Chem. Intermed. **43**, 1723 (2016)
9. M. N. Bhoi, M. A. Borad, E. A. Pithawala, H.D. Patel, Arab. J. Chem. (2016) (in press)
10. M. Kour, S. Paul, J.H. Clark, V.K. Gupta, R. Kant, J. Mol. Catal. A: Chem. **411**, 299 (2016)
11. P.K. Sahu, P.K. Sahu, S.K. Gupta, D.D. Agarwal, Ind. Eng. Chem. Res. **53**, 2085 (2014)
12. M.M. Heravi, E. Hashemi, Y.S. Beheshtiha, K. Kamjou, M. Toolabi, N. Hosseintash, J. Mol. Catal. A: Chem. **392**, 173 (2014)
13. A.B. Atar, Y.S. Jeong, Y.T. Jeong, Tetrahedron **70**, 5207 (2014)
14. L. Nagarapu, H.K. Gaikwad, J.D. Palem, R. Venkatesh, R. Bantu, B. Sridhar, Synth. Commun. **43**, 93 (2013)
15. P.K. Sahu, P.K. Sahu, R. Jain, R. Yadav, D.D. Agarwal, Catal. Sci. Technol. **2**, 2465 (2012)
16. P.K. Sahu, P.K. Sahu, J. Lal, D. Thavaselvam, D.D. Agarwal, Med. Chem. Res. **21**, 3826 (2012)
17. A. Shaabani, A. Rahmati, S. Naderi, Bioorg. Med. Chem. Lett. **15**, 5553 (2005)

18. F.P. Ma, P.H. Li, B.L. Li, L.P. Mo, N. Liu, H.J. Kang, Y.N. Liu, Z.H. Zhang, *Appl. Catal. A* **457**, 34 (2013)
19. V. Polshettiwar, R. Luque, A. Fihri, H. Zhu, M. Bouhrara, J.M. Basset, *Chem. Rev.* **111**, 3036 (2011)
20. R. Hudson, V. Chazelle, M. Bateman, R. Roy, C.J. Li, A. Moores, A.C.S. Sustain, *Chem. Eng.* **3**, 814 (2015)
21. R.B. Nasir Baig, R.S. Varma, *Ind. Eng. Chem. Res.* **53**, 18625 (2014)
22. J. Safari, L. Javadian, *RSC Adv.* **4**, 48973 (2014)
23. D. Wang, D. Astruc, *Chem. Rev.* **114**, 6949 (2014)
24. T.K.H. Ta, M.T. Trinh, N.V. Long, T.T.M. Nguyen, T.L.T. Nguyen, T.L. Thuoc, B.T. Phan, D. Mott, S. Maenosono, H. Tran-Van, *Colloids Surf. A: Physicochem. Eng. Asp.* **504**, 376 (2016)
25. K. Khoshnevisan, M. Barkhi, D. Zare, D. Davoodi, M. Tabatabaei, *Synth. React. Inorg. Met.-Org. Chem.* **42**, 644 (2012)
26. V.A.J. Silva, P.L. Andrade, M.P.C. Silva, L.D.L.S. Valladares, J.A. Aguiar, *J. Magn. Magn. Mater.* **343**, 138 (2013)
27. S. Zhang, H. Niu, Z. Hu, Y. Cai, Y. Shi, *J. Chromatogr. A* **1217**, 4757 (2010)
28. B.Y. Chen, J.H. Qiu, H.X. Feng, *Int. J. Miner. Metall. Mater.* **23**, 234 (2016)
29. M. Liu, H. Jin, E. Uchaker, Z. Xie, Y. Wang, G. Cao, S. Hou, J. Li, *Nanotechnology* **28**, 155603 (2017)
30. A.M. Jubb, H.C. Allen, A.C.S. Appl. Mater. Interfaces. **2**, 2804 (2010)
31. A. Alizadeh, M.M. Khodaei, M. Beygzadeh, D. Kordestani, M. Feyzi, *Bull. Korean Chem. Soc.* **33**, 2546 (2012)
32. M.S. Moorthy, Y. Oh, S. Bharathiraja, P. Manivasagan, T. Rajarathinam, B. Jang, T.T.V. Phan, H. Jang, J. Oh, *RSC Adv.* **6**, 110444 (2016)